

Modelling of propeller shaft dynamics at pulse load

Andrzej Grządziela, Assoc. Prof.
Polish Naval University

ABSTRACT



The article discusses a method of modelling of propeller shaft dynamics at the presence of virtually introduced underwater detonation effects. The propeller shaft model has four degrees of freedom, which provides opportunities for introducing shaft displacements and rotations similar to those observed in a real object. The equations of motion, taking into account the action of external agents, were implemented to the Matlab SIMULINK environment. The obtained time-histories and their spectra were compared with the experimental results of the tests performed on the marine testing ground. The performed model identification confirmed its sensitivity to changing parameters of motion and external actions.

Keywords :

INTRODUCTION

Modelling of technical machines and devices is nowadays done in the form of mathematical and physical models of canonical equations, or virtual 3D tools. Both methods return comparable results, and selecting one of them is determined by an individual approach to the problem, or past experience and habits of a research worker. A basic goal of modelling for diagnostic purposes is to be able to predict failure symptoms, both of primary and secondary nature. The application of static or dynamic loads makes it possible to shorten considerably the time and reduce significantly the cost of the investigations. An important property of the modelling is the ability to introduce complex virtual damages, which in practice either occur rarely, or their occurrence leads to rapid destruction of the machine or group of machines. The modelling aims at finding a group of sensitive symptoms, which uniquely interpret changes of technical state of the machine. The created set of symptoms, tested on a real object, makes a good basis for fast and easy implementation of the vibration based diagnostic system.

The article analyses modes of free vibration of the propeller shaft in the ANSYS environment, and the model of action of underwater detonation, understood as the right-hand side of the second-type Lagrange equation. The ability to introduce virtual damages, such as shaft line axis misalignment, for instance, makes it possible to obtain a sensitive, diagnostic oriented model of the propeller shaft. The following actions were introduced to the proposed dynamic model [2]:

- main engine driving torque
- screw propeller anti-torque
- axial thrust force

- the action resulting from changes in relative positions of load-carrying bearings and thrust bearings in the shaft line
- the action of the hydrodynamic pressure generated by an underwater detonation.

3D MODELLING

The analysis of the propeller shaft dynamics bases on a 3D model worked out in SOLID Works environment and analysed in the ANSYS environment – see Fig. 1. The performed analyses aimed at obtaining the information on free vibration modes of the shaft, with further identification of possible threats during its operation. The results of the analyses of four initial free vibration modes are collected in Tab. 1. These results confirm an opinion that during the operation of a real propulsion system the propeller shaft, working within the range of $n_{ps} = 150 \div 900$ rev/min, is subject to the appearance of resonances.

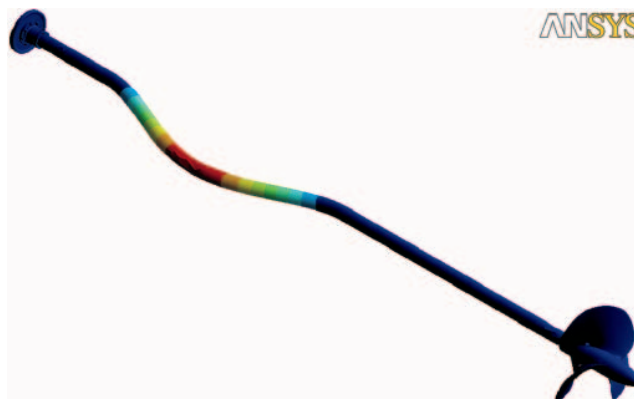


Fig. 1. Sample free vibration mode observed in the analysed propeller shaft

Tab. 1. Analysis of four initial free vibration modes of the shaft

Mode (vibration mode number)	Analysed degree of freedom	Frequency [Hz]	Shaft revolutions [rev/min]
1	Axial. torsional - free Axial - fixed	7.8386	470.30
2	Axial. torsional - free Axial - fixed	7.8529	471.17
3	Axial. torsional - free Axial - fixed	23.961	1437.6
4	Axial. torsional - free Axial - fixed	24.023	1441.4

DYNAMIC MODEL OF THE SHAFT LINE

In the propeller shaft model the driving torque of the internal combustion piston engine is transmitted via the reduction gear to the constant-pitch propeller. The model meets the following requirements:

- ★ makes it possible to introduce the action of external agents
- ★ reveals sensitivity to changing parameters of propeller shaft motion
- ★ reveals sensitivity to propeller shaft axis misalignment
- ★ reveals no sensitivity of the coaxiality symptom to disturbances coming from the environment
- ★ preserves the compliance of the spectral structure in the frequency domain with the results of measurements done on a real object.

The propeller shaft model was an object of simulation tests to check its sensitivity to the action of external agents and compliance with the behaviour of the object in the conditions of the simulated environmental action [5]. The proposed model is nonlinear, and an attempt to describe it by linearisation of actions is unacceptable as it may lead to incorrect conclusions resulting from possible superposition of the effects observed in linear systems [3]. Since in the equations of motion the time is represented explicitly, this system is non-autonomous. A scheme of the reactions on supports at the presence of the external actions is given in Fig. 2.

The kinetic energy of the presented system was written as:

$$E_k = \frac{1}{2} I_N \dot{\varphi}_N^2 + \frac{1}{2} I_{SR} \dot{\varphi}_{SR}^2 + \frac{1}{2} m_I (\dot{v}_I^2 + \dot{h}_I^2) + \frac{1}{2} m_{II} (\dot{v}_{II}^2 + \dot{h}_{II}^2) + \frac{1}{2} m_{SR} (\dot{v}_{SR}^2 + \dot{h}_{SR}^2) + \frac{1}{2} m_N (\dot{v}_N^2 + \dot{h}_N^2) \quad (1)$$

Then, the potential energy of the system was written as:

$$E_p = \frac{1}{2} k_{Ns} \varphi_N^2 + \frac{1}{2} k_{ws} (\varphi_{SR} - \varphi_N)^2 + \frac{1}{2} k_{Ig} (h_I^2 + v_I^2) + \frac{1}{2} k_{IIg} (h_{II}^2 + v_{II}^2) + \frac{1}{2} k_{IIIg} (h_{III}^2 + v_{III}^2) + \frac{1}{2} k_{IVg} (h_{SR1}^2 + v_{SR1}^2) \quad (2)$$

And, finally, the dispersed energy was written as:

$$E_R = \frac{1}{2} c_{ws} (\dot{\varphi}_{SR} - \dot{\varphi}_N)^2 + \frac{1}{2} c_{Ts} \dot{\varphi}_{SR}^2 + \frac{1}{2} c_{Ie} (\dot{h}_I^2 + \dot{v}_I^2) + \frac{1}{2} c_{IIe} (\dot{h}_{II}^2 + \dot{v}_{II}^2) + \frac{1}{2} c_{IIIe} (\dot{h}_{III}^2 + \dot{v}_{III}^2) + \frac{1}{2} c_{IVe} (\dot{h}_{SR1}^2 + \dot{v}_{SR1}^2) \quad (3)$$

The external actions of the drive, understood as the driving torque and the required propeller torque, were given as:

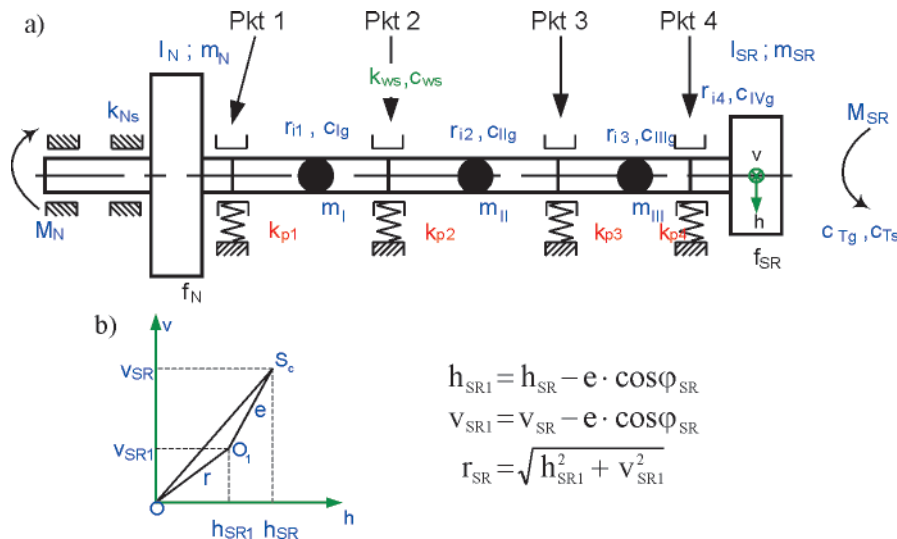


Fig. 2. Scheme of the analysed propeller shaft

where the symbols used in the formulas stand for:

- | | | | |
|--------------------------------------|---|--------------------------------------|---|
| $I_N; m_N$ | – reduced moment of inertia and reduced mass of the driving part | $k_{ws}; c_{ws}$ | – shaft stiffness and torsional damping |
| $I_{SR}; m_{SR}$ | – reduced moment of inertia and reduced mass of the driven part (screw) | $\varphi_N; \varphi_{SR}$ | – rotation angles of the drive and the screw, respectively |
| $M_N; M_{SR}$ | – driving torque and anti-torque (on screw) | $h_{SR}; v_{SR}$ | – horizontal and vertical coordinate of the gravity centre S_c (taking into account shaft deflection) |
| $m_I; m_{II}; m_{III}$ | – reduced masses of shaft elements between successive supports | $h_{SR1}; v_{SR1}$ | – horizontal and vertical coordinate of the rotation centre O_1 |
| k_{Ns} | – torsional stiffness of the drive | $h_N; h_I; h_{II}; v_N; v_I; v_{II}$ | – horizontal and vertical coordinates for masses $m_N; m_I; m_{II}$ |
| $r_{i1}; r_{i2}; r_{i3}; r_{i4}$ | – transverse stiffness coefficients of shaft elements between successive supports | $c_{Tg}; c_{Ts}$ | – water damping resistance: transverse (neglected) and torsional. |
| $c_{Ig}; c_{IIg}; c_{IIIg}; c_{IVg}$ | – transverse dampings of shaft elements between successive supports | | |

$$Q = M_N - M_{sr} \quad (4)$$

Calculating the stiffness k requires solving the statically undeterminable system, which was done using the method of impact coefficients α_{ij} (and coefficients $r_{ij} = f(\alpha_{ij})$ depending on them). In the first step, making use of the equation of three moments and the Wierieszczagin method, the impact coefficients were determined in a general form:

$$\alpha_{k-1,k} = \alpha_{k,k-1} = \frac{I_k}{6EJ_k} \quad (5)$$

$$\alpha_{k,k} = \frac{1}{3} \left(\frac{I_k}{EJ_k} + \frac{I_{k+1}}{EJ_{k+1}} \right) \quad (6)$$

$$\alpha_{k+1,k} = \alpha_{k,k+1} = \frac{I_{k+1}}{6EJ_{k+1}} \quad (7)$$

Then, by rearranging the general formula (in the matrix form) $y_j = \alpha_{ij} S_i$ to the form $S_j = r_{ij} y_j$ the coefficient r_{ij} was determined (taking into account that some matrix elements are equal to zero):

$$\begin{bmatrix} S_1 \\ S_2 \\ S_3 \\ S_4 \end{bmatrix} = \begin{bmatrix} a_{11} & a_{12} & 0 & 0 \\ a_{21} & a_{22} & a_{23} & 0 \\ 0 & a_{32} & a_{33} & a_{34} \\ 0 & 0 & a_{43} & a_{44} \end{bmatrix}^{-1} \begin{bmatrix} y_1 \\ y_2 \\ y_3 \\ y_4 \end{bmatrix} \quad (8)$$

After using the second type Lagrange equations and introducing coefficients r_{ij} to these equations we arrived at Equations (9) which describe the vibrational motion of the propeller shaft. These equations were introduced to the Matlab SIMULINK environment – Fig. 3. Then, the model was complemented by the actions of virtual external agents, which can act individually or in a coupled form. The obtained simulation results refer to the following issues:

- ✦ the analysis of propeller shaft vibrations in stationary conditions

- ✦ the analysis of the system response to individually introduced external dynamic disturbances, such as changes of parameters of coaxiality and underwater detonation pulse
- ✦ the analysis of system response to external dynamic disturbances introduced in a coupled form, for instance for assumed changing coaxiality parameters at the presence of the underwater detonation pulse.

$$\begin{aligned} I_N \ddot{\phi}_N + c_{ws} (\dot{\phi}_N - \dot{\phi}_{SR}) + k_{NS} \phi_N + k_{ws} (\phi_N - \phi_{SR}) &= M_N \\ m_I \ddot{h}_I + c_{Ig} \dot{h}_I + r_{11} h_I + r_{12} h_{II} + r_{13} h_{III} + r_{14} h_{SR} &= 0 \\ m_I \ddot{v}_I + c_{Iv} \dot{v}_I + r_{11} v_I + r_{12} v_{II} + r_{13} v_{III} + r_{14} v_{SR} &= 0 \\ m_{II} \ddot{h}_{II} + c_{IIg} \dot{h}_{II} + r_{21} h_I + r_{22} h_{II} + r_{23} h_{III} + r_{24} h_{SR} &= 0 \\ m_{II} \ddot{v}_{II} + c_{IIv} \dot{v}_{II} + r_{21} v_I + r_{22} v_{II} + r_{23} v_{III} + r_{24} v_{SR} &= 0 \\ m_{III} \ddot{h}_{III} + c_{IIIg} \dot{h}_{III} + r_{31} h_I + r_{32} h_{II} + r_{33} h_{III} + r_{34} h_{SR} &= 0 \\ m_{III} \ddot{v}_{III} + c_{IIIv} \dot{v}_{III} + r_{31} v_I + r_{32} v_{II} + r_{33} v_{III} + r_{34} v_{SR} &= 0 \\ I_{SR} \ddot{\phi}_{SR} + c_{ws} (\dot{\phi}_{SR} - \dot{\phi}_N) + c_{Ts} \dot{\phi}_{SR} + c_{IIIg} (\dot{h}_{SR} \sin \phi_{SR} + & \\ - \dot{v}_{SR} \cos \phi_{SR} + e^2 \dot{\phi}_{SR}) + k_{ws} (\phi_{SR} - \phi_N) + & \\ + r_{44} (h_{SR} \sin \phi_{SR} - v_{SR} \cos \phi_{SR}) &= M_{SR} \\ m_{SR} \ddot{h}_{SR} + c_{IVg} (\dot{h}_{SR} + \dot{\phi}_{SR} \sin \phi_{SR}) + r_{41} h_I + r_{42} h_{II} + r_{43} h_{III} + & \\ + r_{44} (h_{SR} - e \cos \phi_{SR}) &= 0 \\ m_{SR} \ddot{v}_{SR} + c_{IVv} (\dot{v}_{SR} - \dot{\phi}_{SR} \cos \phi_{SR}) + r_{41} v_I + r_{42} v_{II} + & \\ + r_{43} v_{III} + r_{44} (v_{SR} - e \sin \phi_{SR}) &= 0 \end{aligned} \quad (9)$$

The calculations performed in the Matlab SIMULINK environment aimed at iterative introduction of changes of dynamic parameters describing the operation of the propeller

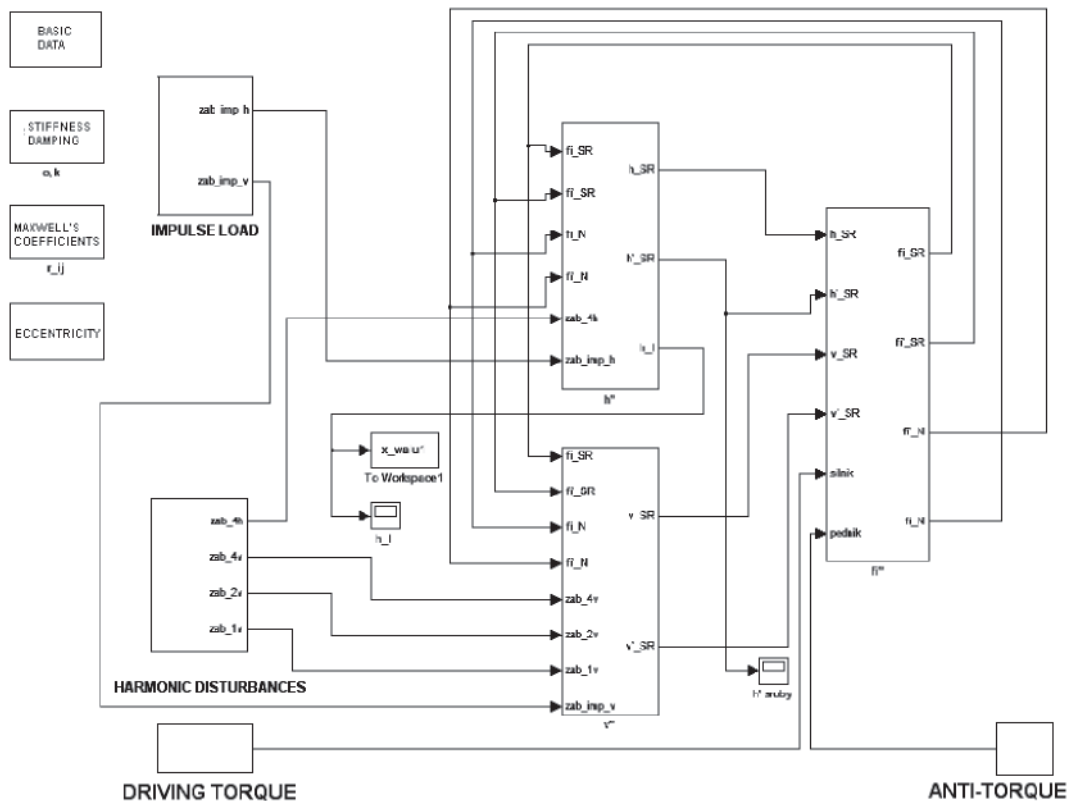


Fig. 3. Starting block of the propeller shaft model in the Matlab SIMULINK environment

shaft model in the simulated real conditions. The model components included the driving torque and anti-torque, changes in the displacement of the propeller shaft axis, and the pulse load coming from an underwater detonation. The underwater detonation model assumed the existence of three successive gas bubble pulses [1,4].

Selected sample simulations of the vibration acceleration spectra recorded at point 2 at the presence of environmental action are given in Fig. 4, while Fig. 5 additionally includes the underwater detonation.

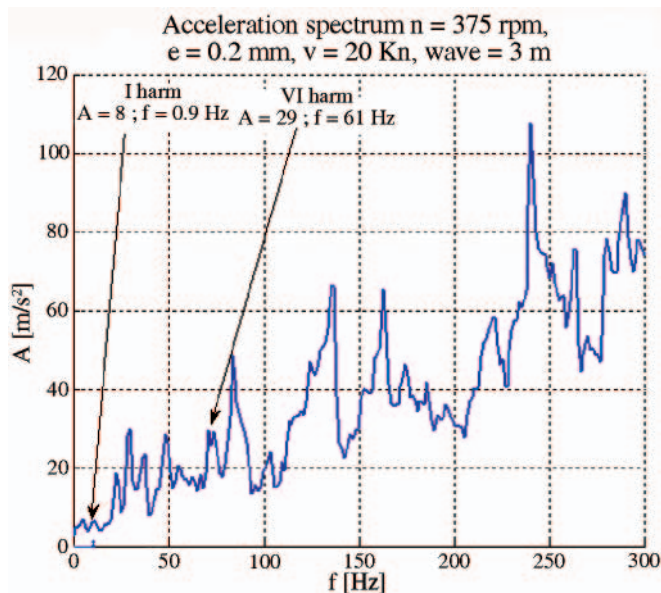


Fig. 4. Simulated transverse vibration spectrum at point 2 for $n_{ps} = 375$ rev/min, $P = 0.2$ mm, $\Delta K = 0^\circ$ and $\zeta = 3$ m

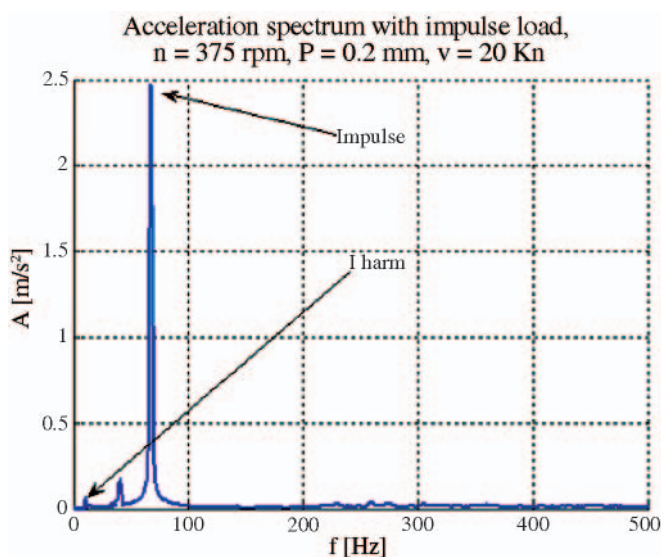


Fig. 5. Simulated transverse vibration spectrum at point 2 for $n_{ps} = 375$ rev/min $\Delta K = 0^\circ$, $\zeta = 5$ m, and detonation pulse $i_d = 50$ g

Fig. 6 shows the simulated action of the underwater detonation at point 1 of the propeller shaft model, done for two distances of the detonation epicentre from the ship hull. The transverse vibration spectra of the propeller shaft loaded with the underwater detonation pulse suggest the existence of a remarkable effect of the distance from the detonation epicentre on the vibration acceleration at the examined point. The nature of the pulse load makes use of the pulse load model [1,4].

In order to illustrate the sensitivity of the model to changes in shaft line misalignment, in Fig. 7 are shown selected spectra of vibration velocities which were recorded at point 2, along V-axis, for course and wave amplitude parameters equal to

$\Delta K = 0^\circ$ and $\zeta = 5$ m, respectively, and for the propeller shaft rotational speed $n_{ps} = 570$ rev/min, for shaft axis displacements $P = 0.2$ mm and $P = 0.5$ mm.

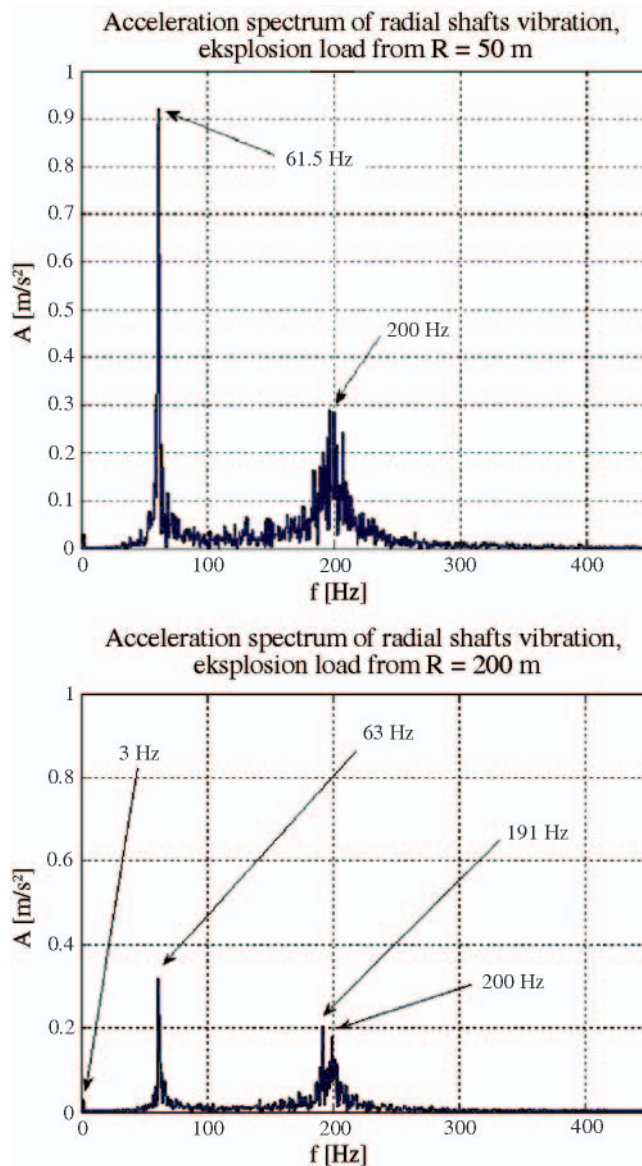


Fig. 6. Simulated transverse vibration acceleration spectra at point 1 for the charge mass $m = 40$ kg blowing at a distance $R = 50$ m and $R = 200$ m

The obtained results confirm the unique effect of shaft axis displacements on the structure and characteristic parameters of the modelled spectrum.

IDENTIFYING THE PROPELLER SHAFT MODEL

The presented dynamic model of the propeller shaft was loaded with virtual loads, including coupled loads, in order to check model applicability to technical diagnostics purposes. The basic criterion for the model compliance with the real object is the compliance of corresponding spectra in frequency domain for different shaft revolutions in stationary conditions [3]. A sample analysis of the results of simulation is given in Figs. 8a and 8b. Changes in the shaft rotational speed which were assumed in the model have resulted in the increase of frequency of the basic harmonic and the sixth harmonic, being an identified symptom of shaft axis misalignment, like in the investigations of a real object. At the same time, the value of the symptom corresponding to the shaft axis displacement by $P = 0.1$ mm increases with increasing shaft revolutions.

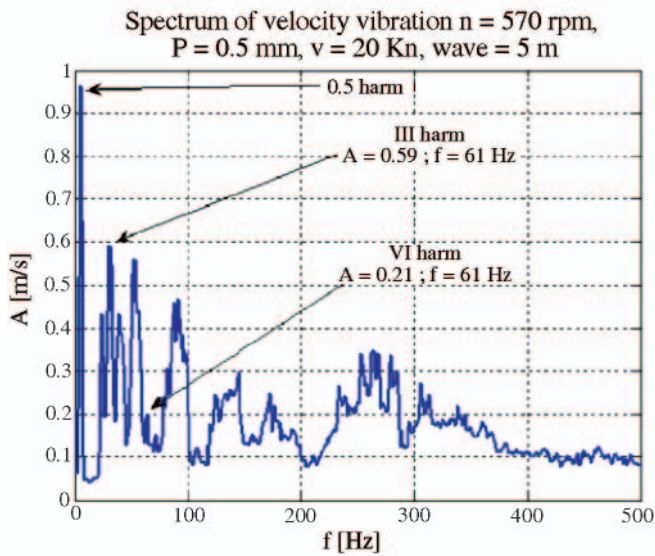
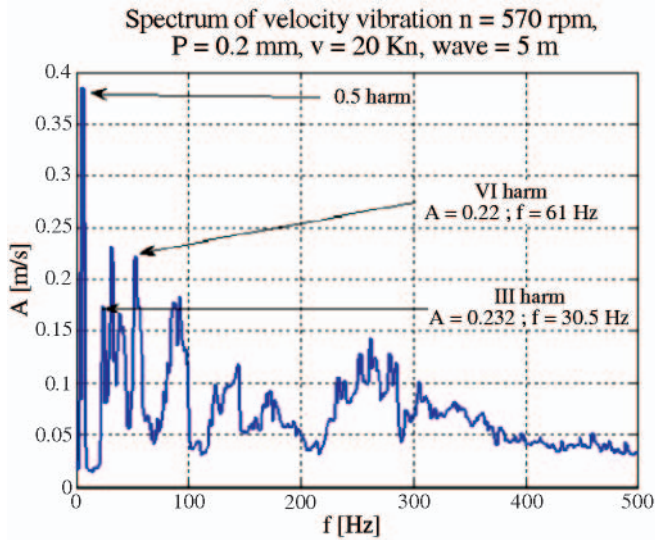


Fig. 7. Simulated transverse vibration velocity spectra at point 2 for assumed propeller shaft axis displacements equal to $P = 0.2$ mm and $P = 0.5$ mm

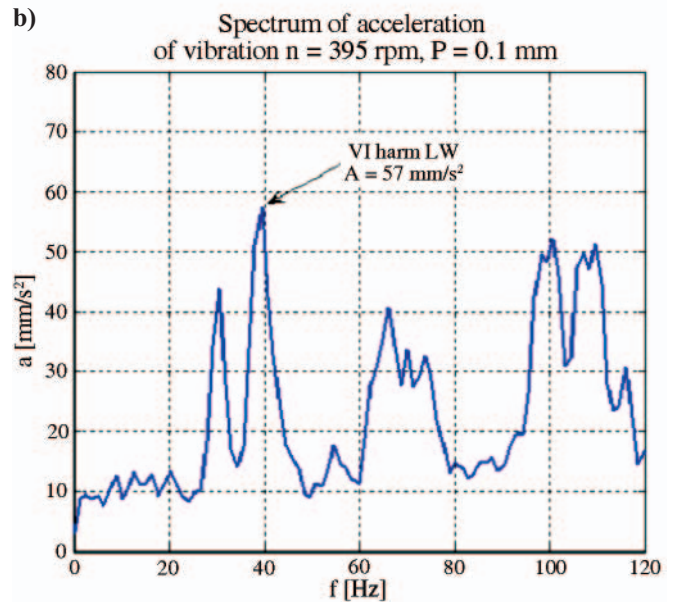
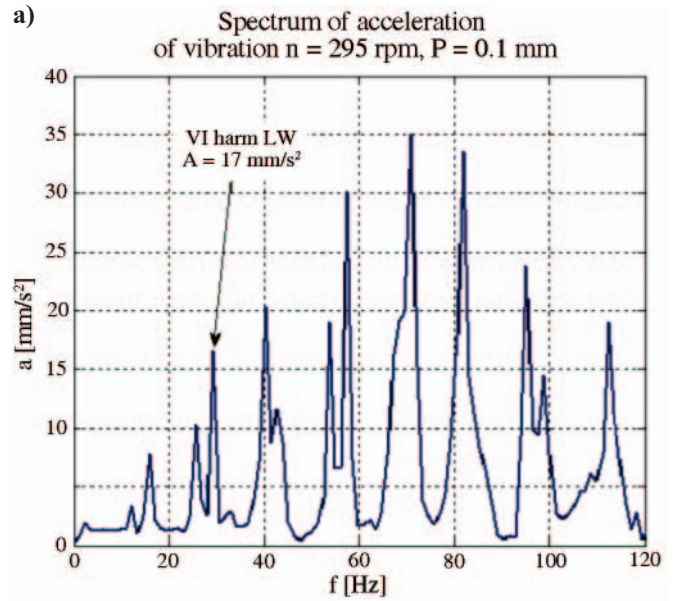
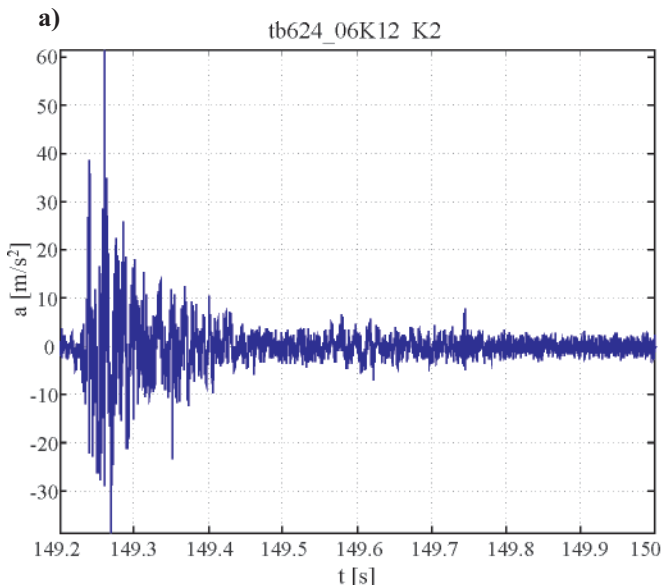


Fig. 8. a) simulated vibration acceleration spectrum for shaft revolutions $n_{ps} = 295$ rev/min at axis displacement $P = 0.1$ mm; b) simulated vibration acceleration spectrum for shaft revolutions $n_{ps} = 395$ rev/min at axis displacement $P = 0.1$ mm

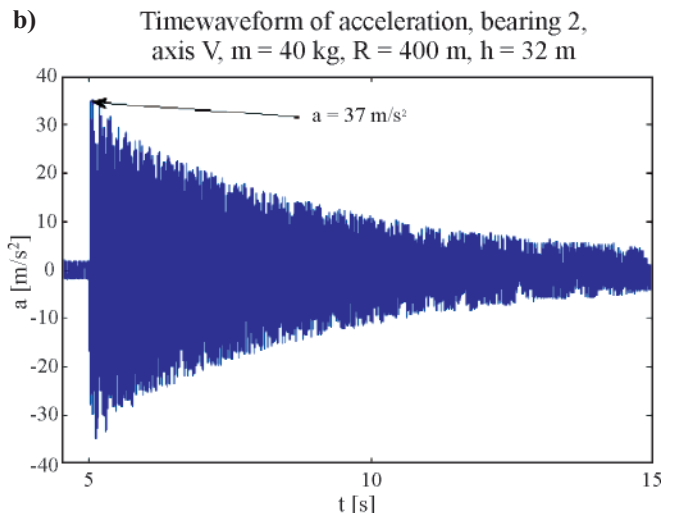


Fig. 9. a) real vibration acceleration time-history recorded during underwater detonation; b) simulated vibration acceleration time-history during underwater detonation

The identification of elastic shaft deformations provoked by an underground detonation is shown in Figs. 9a and 9b. The results measured on a real object were obtained on the marine testing ground after detonating the TNT blowing charge of $m = 40$ kg at a distance of $R = 400$ m and the depth of $h = 32$ m [4]. The simulated detonating action which was introduced to the model consisted of 3 successive pulses, according to the Cole relation [1]. The elastic deformation is best visible when comparing the time-histories of vibration accelerations. Like a real curve, the simulated vibration acceleration time-history is intensively damped, which testifies to the self-centring of the propeller shaft and the elastic nature of the deformation.

The next step in model identification consisted in comparing the results of simulations and measurements done on a real object for known shaft misalignment. The levels of the first and sixth vibration velocity harmonics recorded on the reduction gear thrust bearing casing (point 1 in the model) are given in Fig. 10a, while Fig. 10b shows the effect simulated for the assumed axis displacement equal to $P = 0.2$ mm, the same as on the real object.

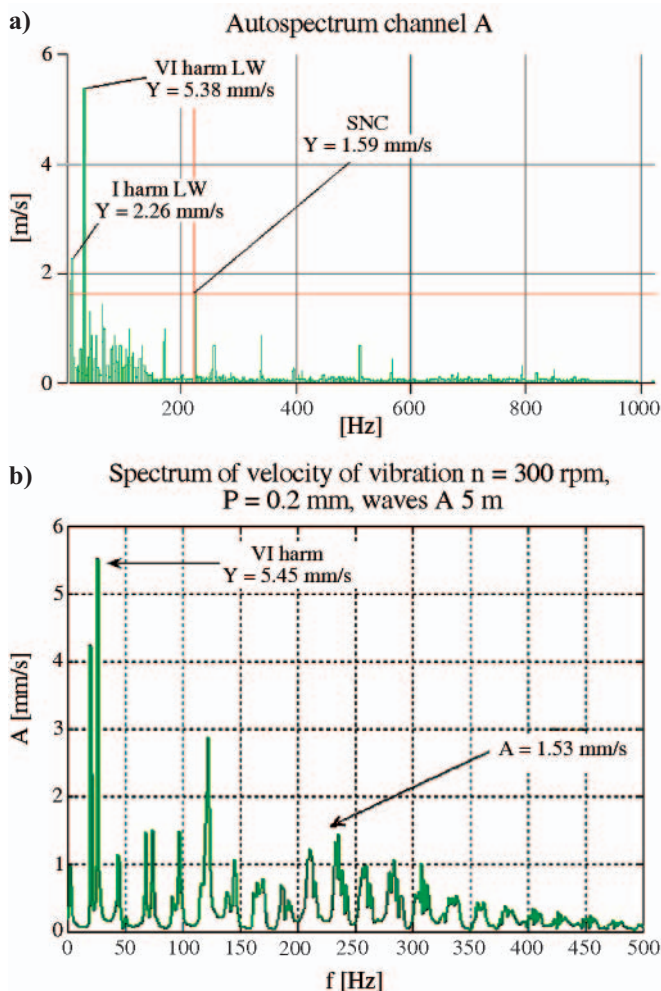


Fig. 10. a) vibration velocity spectrum measured on a real object; b) vibration velocity spectrum simulated using the proposed model

The analysis of the vibration velocity spectra shown in Figs. 10a and 10b reveals that the model preserves similarity of the relations between the basic harmonics. Slight differences in the values of basic components result from the need to use a function which matches the effect of strong nonlinear damping of the water environment, in which a large part of the propeller shaft and the propeller screw are immersed. Identifying the mathematical model consists in such selection of a set of

coefficients or functions that the model solutions are close, within an assumed error tolerance, to the experimental results [8]. Table 2 collects maximum errors recorded when comparing model symptoms with those observed on the real object.

Tab. 2. Maximum errors of model symptoms with respect to the measured results

Symptom	Sixth harmonic of vibration velocity [mm/s]	Sixth harmonic of vibration acceleration [mm/s ²]	Detonation pulse [m/s ²]	First harmonic of vibration velocity [mm/s]
Measured	12.4	5.38	212.2	8.97
Obtained from model	13.6	5.45	206.4	9.78
Maximum relative error	9.67%	1.3%	-2.73%	9.03%

The maximum relative error was assumed not to exceed 10%. Analysing the data collected in Tab. 2 leads to a conclusion that the proposed model is identifiable and sensitive to basic diagnostic parameters.

CONCLUSIONS

A basic goal of modelling is the identification of the diagnostic model. In the reported case, comparing the results of the empirical studies and the simulations has proved good applicability of the proposed model. The obtained results confirmed model sensitivity to changes of the technical state of the object and varying input parameters. A vital property of the model was the insensibility of the axis misalignment symptom to the action of assumed environmental disturbances, such as underwater detonation.

Comparing the measured results with those obtained from the simulations indicates that there is potential space for the use of the results of the simulations in the data base of the on-line monitoring system for propulsion systems used on mine countermeasure vessels. The proposed model is general in nature, which makes it possible to adapt it in similar propeller shaft constructions.

NOMENCLATURE

- a – acceleration
- A – acceleration amplitude
- c_{Ilg} ; c_{IIlg} ; c_{IIIg} ; c_{IVg} – transverse dampings of shaft elements between successive supports
- c_{Tg} ; c_{Ts} – water damping resistance: transverse (neglected) and torsional
- h – depth of detonation
- h_{SR1} ; v_{SR1} – horizontal and vertical coordinate of the rotation centre O_1
- h_N ; h_I ; h_{II} ; v_N ; v_I ; v_{II} – horizontal and vertical coordinates for masses m_N ; m_I ; m_{II}
- h_{SR} ; v_{SR} – horizontal and vertical coordinate of the gravity centre S_c (taking into account shaft deflection)
- i_D – maximum detonation acceleration pulse
- I_N ; m_N – reduced moment of inertia and reduced mass of the driving part
- I_{SR} ; m_{SR} – reduced moment of inertia and reduced mass of the driven part (screw)
- k_{Ns} – torsional stiffness of the propulsion system

k_{ws}, c_{ws}	– stiffness and torsional damping of the shaft
m	– mass
$m_I; m_{II}; m_{III}$	– reduced masses of shaft elements between successive supports
$M_N; M_{SR}$	– driving torque and anti-torque (on screw)
n_{PS}	– propeller shaft rotational speed
P	– axial displacement of the shaft line
$r_{i1}; r_{i2}; r_{i3}; r_{i4};$	– transverse stiffness coefficients of shaft elements between successive supports
R	– distance from detonation epicentre
$\varphi_N; \varphi_{SR}$	– rotation angles of the drive and screw, respectively
ζ	– wave amplitude [m]
$\angle K$	– ship course angle.

BIBLIOGRAPHY

1. Cole R. H.: *Underwater Explosions*. Princeton University Press, Princeton 1948
2. Cudny K.: *Ship shafting. Structures and calculations* (in Polish). Wydawnictwo Morskie. Gdańsk.1990
3. Dąbrowski Z.: *Machine shafts* (in Polish). PWN, Warszawa 1999
4. Grządziela A.: *An analysis of possible assessment of hazards to ship shaft line, resulting from impulse load*. Polish Maritime Research, No. 3/2007, pp. 14 – 17, Gdańsk 2007
5. Grządziela A.: *Dynamic problems of shafts/lines*. Diagnostyka No. 4 vol. 44/ 2007 r, pp. 5 – 10, Olsztyn 2007.

CONTACT WITH THE AUTHOR

Andrzej Grządziela, Assoc. Prof.
Mechanic-Electric Faculty,
Polish Naval University
Śmidowicza 69
81-103 Gdynia, POLAND
e-mail : AGrza@amw.gdynia.pl

Photo: Cezary Spigarski

